FN-715

CONTINUOUS MULTIPLE INJECTIONS AT THE MAIN INJECTOR

K.Y. Ng

*Fermi National Accelerator Laboratory,**
P.O. Box 500, Batavia, IL 60510

(February 2002)

Abstract

Instead of slip-stacking, an alternate method of doubling the linear intensity of the Fermilab Main Injector is discussed. This method makes use of barriers to transfer 12 booster batches from the Fermilab Booster to the Main Injector in 12 consecutive booster cycles, totaling 800 ms. After that adiabatic capture of the beam into 53 MHz buckets can be accomplished in about 10 ms. Because the beam is debunched during the injection process, the cumulative transient beam loading voltage should be much less severe than what will be experienced during slip-stacking.

*Operated by the Universities Research Association, Inc., under contract with the U.S. Department of Energy.

1 INTRODUCTION

In the Fermilab Run IIa, the Fermilab Main Injector is supposed to deliver one booster batch of 5.0×10^{12} protons (84 bunches each containing 6×10^{10} protons) to the targery for the production of anti-protons in a 1.5 s acceleration cycle [1]. In the Run IIb upgrade [2], the number of protons delivered will be doubled. The method to accomplish this is through slip-stacking two booster batches [3]. At the injection total energy of $E = 8.938$ GeV, the Main Injector has a circumference in time of $T_0 = 11.13$ μs, which is exactly 7 booster batches long. The acceleration cycle time in Run IIb will be increased to 2.0 s. This cycle time should be long enough to load the Main Injector with 6 booster batches each of length $T_b = 1.59$ μs, slip-stack one batch to be used for anti-proton production, and extract the other 5 batches for the NuMI neutrino experiment. This cycle is sketched in Fig. 1.

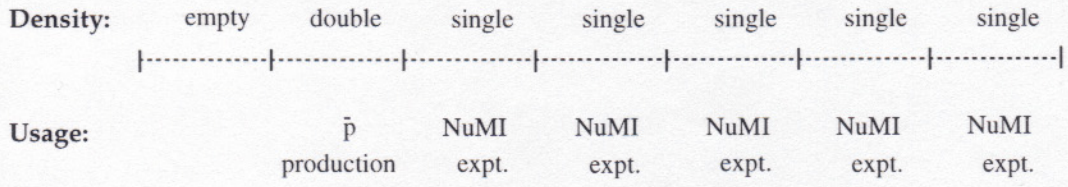

Figure 1: The Main Injector in Run IIb accelerates 5 single-density booster batches for the NuMI neutrino experiment, and one double-density booster batch for anti-proton production. One booster-batch length is left empty. At the injection energy of $E = 8.939$ GeV, one booster-batch length is $T_b = 1.59$ μs and the revolution period of the Main Injector is $T_0 = 7T_b = 11.13$ μs.

Slip stacking had been studied extensively at the CERN Proton Synchrotron (CPS) to double the number of protons per bunch for the production of anti-protons. However, due to the high loss and large increase in final longitudinal and horizontal emittances, the method had never been used in production runs [4]. The main disadvantage of this project is that it involves rf manipulations of intense beams at very low rf voltages resulting in a severe beam loading situation. At Fermilab, we plan on correcting the beam loading with direct rf feedback around the rf cavities in the Main Injector. Simulations show that very large loop gains are needed to remove the beam loading to a sufficient level. The large loop gains are associated with a number of stability issues.

An alternative way to double the density of the proton bunches is through the use of

Table I: Some injection parameters of the Main Injector.

Nominal total energy E	8.9383	GeV
Relativistic γ/β	9.326/0.99448	
Transition gamma	21.8	
Slip factor η	-0.008915	
Revolution period T_0	11.1339	μs
Length of booster batch $T_b = T_0/7$	1.5906	μs
Booster repetition rate	15	Hz

barrier waves. First, inject two booster batches into the Main Injector. Second, introduce two barriers at the ends of the two-batch region. Third, squeeze the barriers to compress the two-batch region to a one-batch length resulting in doubling the longitudinal intensity. Fourth, capture the compressed double-density batch into 53 MHz rf buckets. Finally, fill the next 5 booster lengths with one booster batch each. The result is a double-density batch in the first section for anti-proton production followed by 5 single-batch sections for NuMI neutrino experiment. This method of increasing beam density using barriers has been studied theoretically by Machida [5] and Ng [6], and experimentally at the Brookhaven Alternating Gradient Synchrotron [7]. However, this method has the disadvantage of being too time consuming. In order not to increase the longitudinal emittance of the beam, the bunch compression by barrier squeezing has to be adiabatic. The barrier movement speed $\dot{T}_2$ must be very much less than one half the maximum phase-drifting speed of the particles with largest fractional momentum offset, or [6]

$$|\dot{T}_2| \ll \frac{|\eta\delta|}{2T_0}, \qquad \frac{1}{2}|\eta\delta| \tag{1.1}$$

where η is the slip factor and T_0 the revolution period of the accelerator ring. Thus, for the compression of a booster-batch length T_b, the time required becomes

$$\text{Barrier squeezing time} \gg \frac{2T_b}{|\eta\delta|} \ . \tag{1.2}$$

Using the Main Injector parameters in Table 1, even with a maximum fractional momentum half spread of $\delta = 3.39 \times 10^{-3}$, the barrier squeezing time must be very much larger than 0.36 s. This will lengthen the Main Injector acceleration cycle significantly and is therefore unacceptable.

Another method of doubling beam density by barriers was introduced by Griffin [8]. This is a momentum stacking method which does not require adiabatic bunch compression.

As a result, injection from the Fermilab Booster can proceed batch by batch at the booster cycling rate, and all the 6 batches can have their density doubled in 12 booster cycles. After that the beam will be captured adiabatically into 53 MHz buckets in about 10 ms before acceleration takes place. The whole accelerator cycle should be well within the proposed 2 s. In this paper, we are going to examine this method in detail. Some simulations have been performed.

2 THE INJECTION METHOD

Let us start with a booster batch of protons of length T_b and full fractional momentum spread Δ. This batch, denoted by 1 in Fig. 2(a), is injected into the Main Injection at a *negative* momentum offset, so that the highest fractional momentum offset[†] is δ_{i1} and the lowest fractional momentum offset is $\delta_{i2} = \delta_{i1} - \Delta$. The longitudinal position of the injection is so chosen that the right side of the batch just touches the left side of a square barrier (denoted by B) of width T_1 and magnitude V, which is moving to the left at the speed of $\dot{T}_2 = T_b/(2T_c)$ where T_c is the booster-cycle time. The momentum offset of the batch injection is so chosen that the proton of highest energy on the left side of the batch will drift to the right at the speed of $\frac{1}{2}T_b$ per booster cycle or $-\dot{T}_2$. Thus, after one booster cycle, another batch marked 2 in Fig. 2(b) can be injected again with its right edge touching the left side of the barrier. In other words, at every booster cycle, a new booster batch can be injected with the injection point moved half a booster-batch length to the right. The linear beam density can therefore be doubled.

The only parameter here is the size of the barrier, which is so chosen that after the booster batch emerges from the barrier, the highest and lowest energies of the batch become symmetric about the nominal energy of the accelerator ring. This is necessary because we need to place another stationary barrier on the right side of the moving barrier in order to limit the longitudinal motion of the protons after passing through the moving barrier so as to guarantee empty spaces along the Main Injector for successive batch transfer from the Booster. It will be shown in the Appendix that the injection method described here just depends on the integrated size of the barrier and is independent of its shape. As a result, we denote the size of the barrier by VT_1 and barrier of any shape can be used. However, for

[†]We denote by the subscript 1 the particle at the upper right corner of the batch and 2 the particle at the lower right corner of the batch

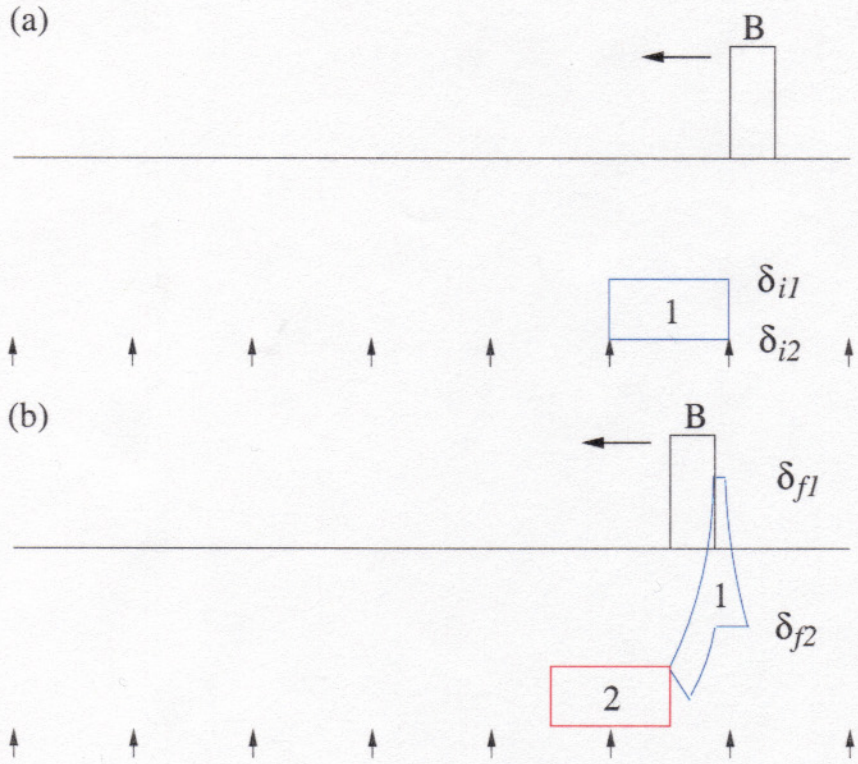

Figure 2: (color) (a) A booster batch (marked 1) is injected at negative momentum offset with the right edge just touching a left-moving barrier (marked B). The vertical arrows are spaced one booster-batch length T_b. (b) After a booster cycle, the barrier moves by half a booster-batch length while all particles in batch 1 drift past the left edge of the barrier. After exiting the barrier, the batch has maximum and minimum momenta, δ_{f1} and δ_{f2}, symmetric about the on-momentum particles. A second booster batch (marked 2) is now injected.

the ease of derivation, we continue to assume a rectangular barrier.

The mathematic determination of VT_1 is as follows. Let us start from the time when the proton at the upper right corner of the batch enters the barrier. After n turns into the barrier, the fractional momentum offset is

$$\delta_{n1} = \delta_{i1} + n\Delta\delta \ , \tag{2.1}$$

where

$$\Delta\delta = \frac{eV}{\beta^2 E} \tag{2.2}$$

is the fractional momentum gained by the particle encountering the barrier per turn, e is the proton charge, E is the on-momentum energy of the protons in the Main Injector, βc its

longitudinal velocity, and c the velocity of light. Suppose this proton exits the barrier in the N_1 turns. Its phase drift in time[‡] towards the right is

$$\int_0^{N_1} \eta T_0(\delta_{i1} + n\Delta\delta)dn \ , \tag{2.3}$$

where η is the slip factor and T_0 is the revolution period. At this moment, the barrier has moved towards the left by the phase $N\dot{T}_2T_0$. Because the width of the barrier is T_1, we must have

$$T_1 - N_1\dot{T}_2T_0 = \int_0^{N_1} \eta T_0(\delta_{i1} + n\Delta\delta)dn \ . \tag{2.4}$$

The turn number N_1 therefore satisfies the quadratic equation

$$N_1^2 + 2N_1\frac{\delta_{i1} - \dot{T}_2/|\eta|}{\Delta\delta} - \frac{2T_1}{\eta T_0\Delta\delta} = 0 \ . \tag{2.5}$$

Noting that the Main Injector is below transition at injection, the solution is

$$N_1 = -\frac{\delta_{i1} - \dot{T}_2/|\eta|}{\Delta\delta} - \sqrt{\left(\frac{\delta_{i1} - \dot{T}_2/|\eta|}{\Delta\delta}\right)^2 - \frac{2T_1}{|\eta|T_0\Delta\delta}} \ . \tag{2.6}$$

Note that the first term on the right is positive while the last term in the square root is negative. Thus both $\pm$ signs before the square root should give a positive turn number N_1. However, when the barrier width goes to zero ($T_1 \to 0$), number of turns to clear the barrier also goes to zero ($N_1 \to 0$). This validates the choice of the negative sign. Substituting into Eq. (2.1), we obtain the final fractional momentum offset of the proton concerned,

$$\delta_{f1} = \delta_{i1} + N_1\Delta\delta = \frac{\dot{T}_2}{|\eta|} - \sqrt{\left(\delta_{i1} - \frac{\dot{T}_2}{|\eta|}\right)^2 - \frac{2T_1\Delta\delta}{|\eta|T_0}} \ . \tag{2.7}$$

The final fractional momentum offset of the proton with the lowest energy is also given by Eq. (2.7) when the substitutions of the subscripts $i1 \to i2$ and $f1 \to f2$ are made. In order that final momentum spreads of the protons to be symmetric about the nominal energy E, we require $\delta_{f1} = -\delta_{f2}$, or

$$\frac{\dot{T}_2}{|\eta|} - \sqrt{\left(\delta_{i1} - \frac{\dot{T}_2}{|\eta|}\right)^2 - \frac{2T_1\Delta\delta}{|\eta|T_0}} = -\left[\frac{\dot{T}_2}{|\eta|} - \sqrt{\left(\delta_{i2} - \frac{\dot{T}_2}{|\eta|}\right)^2 - \frac{2T_1\Delta\delta}{|\eta|T_0}}\right] \ . \tag{2.8}$$

[‡]We denote the phase drift as time arrival ahead of some on-momentum particle. Because the Main Injector at injection is below transition or $\eta < 0$, the phase drift or arrival time is positive for a negative-momentum-offset particle.

Now we substitute for $\delta_{1i} = -\dot{T}_2/|\eta|$, $\delta_{2i} = \delta_{1i} - \Delta$, and express everything in terms of $2\dot{T}_2/|\eta|$. The above equation simplifies to[§]

$$1 - \sqrt{1-A} = \sqrt{(\bar{\Delta}+1)^2 - A}\ , \tag{2.9}$$

where $\Delta = \bar{\Delta}(2\dot{T}_2/|\eta|)$,

$$A = \frac{2T_1\Delta\delta}{|\eta|T_0}\left(\frac{\eta}{2\dot{T}_2}\right)^2\ , \tag{2.10}$$

which is proportional to VT_1, the size of the barrier. We can readily obtain

$$A = \frac{1}{4}(1+\bar{\Delta})^2(\bar{\Delta}+3)(\bar{\Delta}-1)\ , \tag{2.11}$$

or

$$VT_1 = \frac{|\eta|^3\beta^2 ET_0}{32e\dot{T}_2^2}(\delta_{i1}+\delta_{i2})^2\left(\delta_{i1}+\delta_{i2}-\frac{4\dot{T}_2}{|\eta|}\right)\left(\delta_{i1}-\delta_{i2}-\frac{2\dot{T}_2}{|\eta|}\right)\ . \tag{2.12}$$

3 CRITICAL MOMENT

Obviously, a larger initial fractional momentum spread Δ of the beam will lead to a larger final fractional momentum spread. However, when the initial fractional momentum spread is large enough, protons with the highest momentum will acquire so much energy from the moving barrier that their drifting speeds to the left exceed the speed of the moving barrier. The result is that these particles will not be able to emerge from the moving barrier and this injection method fails. This happens when

$$\dot{T}_2 < |\eta|\delta_{f1}\ , \tag{3.1}$$

where δ_{f1} is given by Eq. (2.7), or the expression under the square root of Eq. (2.7) becomes negative. This gives us the critical size of the moving barrier

$$(VT_1)_c = \frac{|\eta|\beta^2 ET_0}{2e}\left(\frac{2\dot{T}_2}{|\eta|}\right)^2\ . \tag{3.2}$$

The same can be inferred by squaring Eq. (2.9) to give

$$\sqrt{1-A} = 1 - \frac{(1+\bar{\Delta})^2}{2}\ , \tag{3.3}$$

[§]Every normalized variable carries a bar.

and notice that the left side is positive semi-definite while the right side can be negative. This lead to the critical value of $A = 1$ which is the expression given by Eq. (3.2) and the corresponding maximum normalized $\bar{\Delta}_c = \sqrt{2} - 1$. Thus the maximum allowable initial full fractional momentum spread of the beam is

$$\Delta_c = \left(\sqrt{2} - 1\right) \frac{2\dot{T}_2}{|\eta|} \,. \tag{3.4}$$

For the Main Injector, these critical numbers are $(VT_1)_c = 3.1421$ kV-μs and $\Delta_c = 0.001109$. The critical half energy spread of the batch is therefore $\Delta E_{\frac{1}{2}c} = \Delta_c \beta^2 E/2 = 4.900$ MeV.

4 GENERALIZED METHOD

In order to incorporate initial full momentum spread of the beam larger than the critical value of $\Delta_c = 0.001109$, the obvious way is to let the barrier move to the left at a higher speed. Let the barrier move to the left at the speed xT_b for each booster cycle of $T_c = 1/15$ s so that $\dot{T}_2 = xT_b/T_c$ ($x = \frac{1}{2}$ in Sec. 2 and 3). To ensure injection for each booster cycle, an injected batch must clear the left edge of the moving barrier in a booster cycle. Therefore, protons in the batch with top energy must drift to the right at the speed of $yT_b/T_c = y\dot{T}_2/x$, with $x + y = 1$. In other words, these top-energy protons at injection must have fractional momentum offset given by

$$\delta_{i1} = -\frac{y\dot{T}_2}{x|\eta|} \,. \tag{4.1}$$

The derivation proceeds in the same way as in Sec. 2. These protons have final fractional momentum offset given by Eq. (2.7) and the equation for the determination of VT_1 is again given by Eq. (2.8). Substituting for the value of δ_{i1} given by Eq. (4.1) and normalizing everything with respect to $2\dot{T}_2/|\eta|$, we obtain, instead of Eq. (2.9),

$$1 - \sqrt{\frac{1}{4x^2} - A} = \sqrt{\left(\frac{1}{2x} + \bar{\Delta}\right)^2 - A} \,, \tag{4.2}$$

where A is still given by Eq. (2.10). Squaring, we get

$$2\sqrt{\frac{1}{4x^2} - A} = 1 - \frac{\bar{\Delta}}{x} - \bar{\Delta}^2 \,. \tag{4.3}$$

To ensure that the right side will not become negative, we obtain the critical condition

$$\bar{\Delta} < \sqrt{\frac{1}{4x^2} + 1} - \frac{1}{2x} \,. \tag{4.4}$$

Putting back the normalization factor $2\dot{T}_2/|\eta| = 2xT_b/(|\eta|T_c)$, we obtain the critical full fractional momentum spread of the beam

$$\Delta_c = \left(\sqrt{x^2+\frac{1}{4}}-\frac{1}{2}\right)\frac{2T_b}{|\eta|T_c} \ . \tag{4.5}$$

Conversely, given a full fractional momentum spread Δ, the speed of the moving barrier must be faster than xT_b/T_c where

$$x = \sqrt{\frac{|\eta|T_c\Delta}{2T_b}\left(\frac{|\eta|T_c\Delta}{2T_b}+1\right)} \ . \tag{4.6}$$

For example, given the barrier moving rate x, and given an initial full momentum spread $\Delta < \Delta_c$, what is the required VT_1 for the moving barrier? This can be obtained by continuing the solution of Eq. (4.3). The final answer is

$$VT_1 = \frac{T_0T_b^2\beta^2E}{2|\eta|T_c^2}\,4x^2A = \frac{T_0T_b^2\beta^2E}{2|\eta|T_c^2}\left(1-\bar{\Delta}\right)\left(1+\bar{\Delta}\right)\left(1-x+x\bar{\Delta}\right)\left(1+x+x\bar{\Delta}\right) \ . \tag{4.7}$$

The critical size of the moving barrier can be obtained easily from Eq. (4.3):

$$A = \frac{1}{4x^2} \ . \tag{4.8}$$

Since A is given by

$$A = \frac{2T_1\Delta\delta}{|\eta|T_0}\left(\frac{|\eta|}{2\dot{T}_2}\right)^2 = \frac{2T_1\Delta\delta}{|\eta|T_0}\left(\frac{|\eta|T_c}{T_b}\right)^2\frac{1}{4x^2} \ , \tag{4.9}$$

the critical size of the moving barrier is independent of x and remains given by

$$(VT_1)_c = \frac{T_0T_b^2\beta^2E}{2|\eta|T_c^2} = 3.1421 \text{ kV-}\mu\text{s} \ . \tag{4.10}$$

At the critical condition, the injection energy offset $\Delta E_{i1} = \delta_{i1}\beta^2E$ and final half energy spread $\Delta E_{f1} = \delta_{f1}\beta^2E$ are plotted in Fig. 3 as functions of initial half energy spread $\Delta E_{\frac{1}{2}i}$. As the initial half energy spread increases, the critical speed of the barrier increases. The top-energy particles will be drifting at the same speed as the barrier and therefore the final half energy spread increases. On the other hand, the drifting of the batch at injection decreases, so does the initial energy offset at injection. For a given barrier speed $\dot{T}_2 = xT_b/T_c$, the critical injection energy offset ΔE_{i1}, critical initial half energy spread $\Delta E_{\frac{1}{2}i}$, and critical

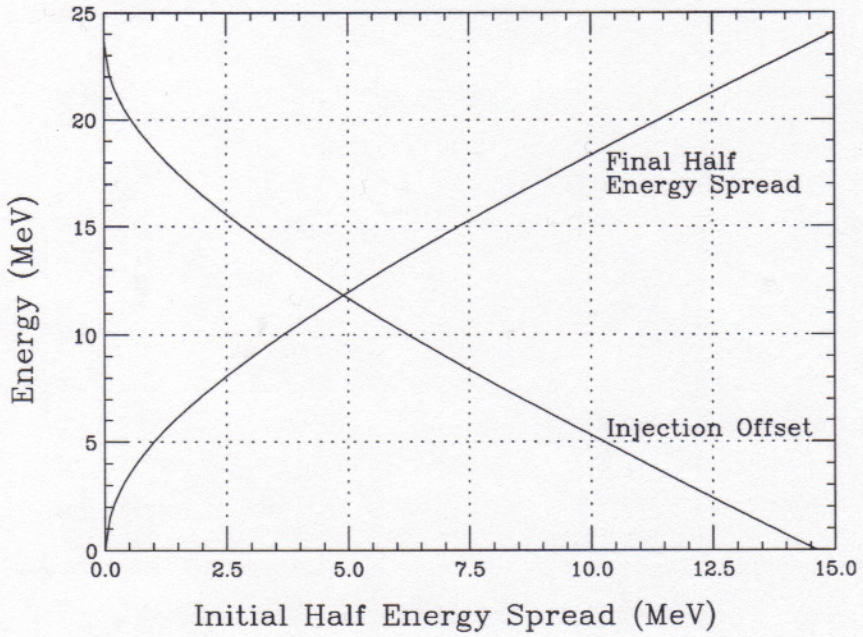

Figure 3: At the critical condition, the initial energy offset at injection $\Delta E_{i1} = \delta_{i1}\beta^2 E$ and final half energy spread $\Delta E_{f1} = \delta_{f1}\beta^2 E$ versus the initial half energy spread of the booster batch.

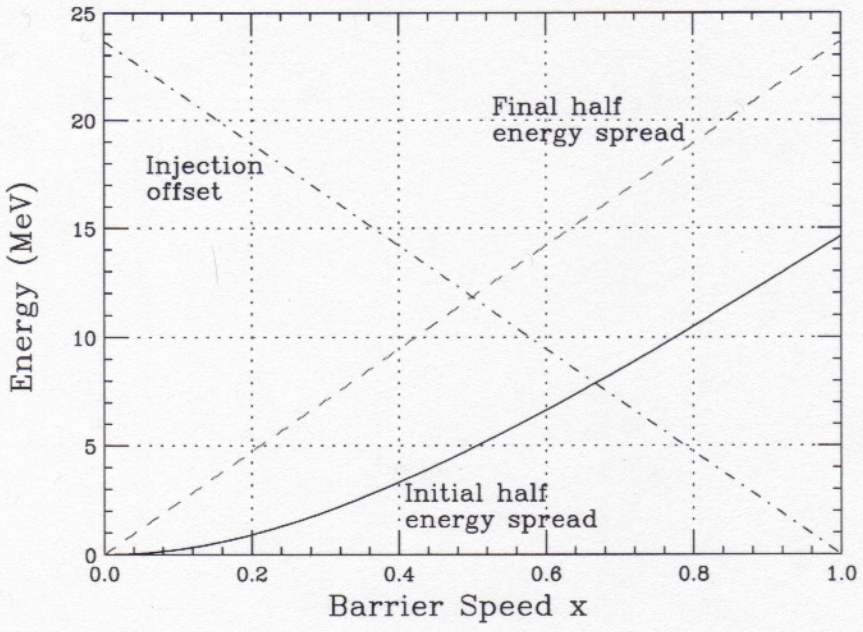

Figure 4: Given a barrier speed, the plot shows the critical initial half energy spread of the booster batch $\Delta E_{\frac{1}{2}i}$, the initial energy offset ΔE_{i1}, and the final half energy offset ΔE_{f1}.

final half energy spread ΔE_{f1} can be looked up in Fig. 4. Thus, if the initial half energy spread $\Delta E_{\frac{1}{2}i}$ is very small, we can perform the injection with a very slow speed for the moving barrier. This allows us to inject at every xT_b along the accelerator ring and we can obtain x^{-1}-fold stacking in the momentum space. The final energy spread will therefore increase by x^{-1} folds.

5 EMITTANCE AND LINEAR DENSITY

When the injection barrier is moving to the left at xT_b per booster cycle, the position of injection along the accelerator ring slips to the left by xT_b for each injection or for each booster cycle. This means that we can inject in the length xT_b a whole batch of length T_b. Or we can inject in the length T_b, $1/x$ batches. Therefore the ratio of emittance by this method and the original emittance is

$$r_e = \frac{\delta_{f1} \times 1}{\frac{\Delta}{2} \times \frac{1}{x}} \ . \tag{5.1}$$

Here, we assume cicumference of the accelerator ring is infinitely long so that injection can be continued for ever. The final momentum offset δ_{f1} is still given by Eq. (2.7) with $\delta_{i1} = -y\dot{T}_2/(x|\eta|)$. Normalizing with respect to $2\dot{T}_2/|\eta|$, we obtain

$$\bar{\delta}_{f1} = \frac{1}{2} - \sqrt{\frac{1}{4x^2} - A} \ . \tag{5.2}$$

With the help of Eq. (4.3), this gives

$$\bar{\delta}_{f1} = \frac{\bar{\Delta}}{2x}(1 + x\bar{\Delta}) \ . \tag{5.3}$$

The emittance-growth ratio becomes

$$r_e = 1 + x\bar{\Delta} = 1 + \frac{|\eta| T_c \Delta}{2T_b} \ . \tag{5.4}$$

It is interesting to see that this emittance growth is independent of x, or the speed at which the barrier moves.

Another important number is the final linear density. When the barrier is moving to the left at the speed of xT_b per booster cycle, we can inject a batch at every length xT_b rather

than at every T_b without the barrier. Thus, the ratio of linear density with barrier to the linear density without barrier is

$$r_d = \frac{1}{x} \,. \tag{5.5}$$

For example, the linear density is doubled when $x = \frac{1}{2}$. For this reason, we should choose the lowest barrier moving speed allowable by the initisl momentum spread of the batch. In other words, given Δ, we should stick to the critical x given by Eq. (4.6) and the critical size $(VT_1)_c$ for the barrier given by Eq. (4.10).

Given an initial half energy spread of the booster batch, the slowest speed $\dot{T}_2 = xT_b/Tc$ of the moving barrier and the emittance increase $r_e - 1$ are plotted in Fig. 5. We see that in order to keep the barrier speed at $\dot{T}_2 = T_b/(2T_c)$ or $x = \frac{1}{2}$, the half energy spread of the booster batch should not exceed $\Delta E_{\frac{1}{2}i} = 4.90$ MeV. We also see that the longitudinal emittance increases linearly with $\Delta E_{\frac{1}{2}i}$ as indicated by Eq. (5.4).

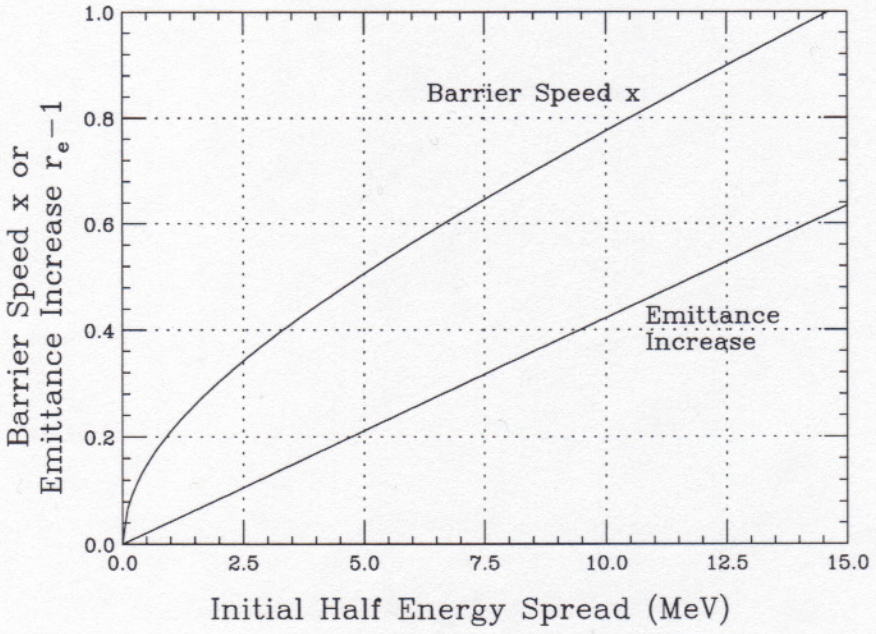

Figure 5: The slowest or critical speed of the moving barrier and the longitudinal emittance increase versus the half energy spread of the booster batch.

6 APPLICATION TO MAIN INJECTOR

At the extraction of the Fermilab Booster, a booster bunch has a bunch area of $\mathcal{A} = 0.10$ eV-s. Since there are $h_B = 84$ bunches at 53 MHz rf in the batch, if they are debunched adiabatically, the half energy spread is only

$$\Delta E = \frac{h_B \mathcal{A}}{T_b} = 2.64 \text{ MeV} . \tag{6.1}$$

However, time-consuming adiabatic debunching in the Booster is not possible because the Booster is a 15 Hz rapid-cycling machine. As a result, the rf voltage $V_{\rm rf}$ must be lowered gradually after transition crossing to a small value near extraction. This process can also encouter problems, because the accerating bucket will become smaller and beam loss can occur.

The half energy spread of a booster bunch is

$$\Delta E = \sqrt{\frac{\omega_s A \beta^2 E}{\pi \eta}} , \tag{6.2}$$

where

$$\omega_s = \omega_0 \sqrt{\frac{h\eta V_{rmrf}}{2\pi\beta^2 E}} \tag{6.3}$$

V_{rf}

ω_s is the angular synchrotron frequency and $\omega_0/(2\pi) = 1/T_b$ is the Booster revolution frequency. At extraction, the energy E of a particle together with its Lorentz factors are the same as those for the Main Injector at injection and are listed in Table I. The Booster has a transition gamma of $\gamma_t = 5.6$, the slip factor at extraction is therefore $\eta = 0.02087$. Thus if the rf voltage can be lowered to $V_{\rm rf} = 10$ kV, the half energy spread of the bunch is $\Delta E = 5.47$ MeV. This is still larger than the critical half energy spread of $\Delta E_{\frac{1}{2}c} = 4.900$ MeV, if we would like the barrier to move at the speed given by $x = \frac{1}{2}$.

Another method of reducing the half energy spread is to introduce higher harmonic cavities into the Booster rf system so that the bunch can be made more rectangular like. The rf wave becomes

$$V(\theta) = V_{\rm rf} \left[\sin\theta - r \sin m\theta\right] \tag{6.4}$$

where θ is the rf phase, m the higher harmonic multiple and $-rV_{\rm rf}$ the voltage of the higher harmonic cavity. If we let $r = 1/m$, the rf potential becomes quartic at small amplitude. The bunch is therefore lengthened with its energy spread lowered. For a $\mathcal{A} = 0.11$ eV-s bunch

at $V_{\rm rf} = 9.725$ kV, the half energy spread is reduced [9] from $\Delta E = 5.43$ MeV to 5.0 MeV with the introduction of a $m = 3$ higher harmonic cavity. For a $\mathcal{A} = 0.10$ eV-s bunch at $V_{\rm rf} = 4.8$ kV, the half energy spread is reduced from $\Delta E = 4.56$ MeV to 3.7 MeV with the introduction of a $m = 2$ higher harmonic cavity.

The momentum spread of the booster bunch can also be reduced before extraction using a bunch rotation by one quarter of a synchrotron oscillation. At this moment, longitudinal coupled-bunch instabilities are observed near extraction. Bunch rotation of an oscillating bunch will not necessarily produce a bunch of small momentum spread. Thus, the coupled-bunch instabilities must be cured by either de-Qing the offensive modes inside the booster cavities and/or repairing the longitudinal damper which has not been working properly at the present. We are confident that the half energy spread of a booster batch can be made below the critical $\Delta E_{\frac{1}{2}C} = 4.900$ MeV before extraction.

6.1 SIMULATIONS

We perform simulations for this injection method from the Booster to the Main Injector at the critical condition for barrier movement of $\frac{1}{2}T_b$ per Booster cycle or $x = \frac{1}{2}$, or $\dot{T}_2 = T_b/(2T_c) = 1.193 \times 10^{-5}$. The half energy spread of the booster batch is assumed to be $\Delta E_{\frac{1}{2}i} = 4.900$ MeV initially, exactly the critical value. Particles with the highest energy are injected with the offset of $\Delta E_{i1} = -\dot{T}_2\beta^2 E/|\eta| = -11.8285$ MeV while particles with the lowest energy are injected with offset $\Delta E_{i2} = \Delta E_{i1} - 2\Delta E_{\frac{1}{2}i} = -21.6276$ MeV. After exciting the moving barrier, their final energy offsets are $\Delta E_{f1} = -\Delta E_{i1} = 11.8285$ MeV and $\Delta E_{f2} = -\Delta E_{f1} = -11.8285$ MeV. These are tabulated in Table II. Thus, the energy spread has been increased by the factor $\Delta E_{f1}/\Delta E_{\frac{1}{2}i} = 11.8285/4.8995 = 2.419$ and this is also the ratio of the final longitudinal emittance to the initial longitudinal emittance.

The moving barrier has its $VT_1 = 3.1421$ kV-μs, the critical value is given by Eq. (4.10). It is advisable to have the barrier voltage as high as possible, so that its width can be made narrow to allow for more space for injection. We choose $T_1 = 1.0$ μs so that $V = 3.1421$ kV. We start by placing this barrier with its left edge at a position which we denote by $6.5T_b$ along the Main Injector as illustrated in top plot of Fig. 6, where we also see the first batch injected with energy offset at the position between $5.5T_b$ and $6.5T_b$. Another stationary barrier is placed with is right edge at the $7.0T_b$ point of the ring to block particles with negative energies to drift to left side of the moving barrier so as to ensure space for new injections.

Table II: Some parameters in the simulations of this injection method from Booster to Main Injector.

$\dot{T}_2 = T_b/T_c$	1.193×10^{-5}	
Half energy spread $\Delta E_{\frac{1}{2}i}$	4.900	MeV
Injection energy offset top of bunch ΔE_{i1}	-11.8285	MeV
bottom of bunch ΔE_{i1}	-21.6276	MeV
Final half energy spread $\Delta E_{f1,f2}$	± 11.8285	MeV
Moving barrier VT_1	3.1421	kV-μs
Minimum reflection barrier VT_1	0.7855	kV-μs

From the Hamiltonion in Eq. (A.2) or Eq. (A.5), the minimum size of this reflection barrier is

$$VT_1 = \frac{|\eta| T_0 \Delta E_{f1}^2}{2\beta^2 E} = 0.7855 \text{ kV-}\mu\text{s}. \tag{6.5}$$

To ensure that the barrier will catch all the right-drifting particles, we choose $VT_1 = 0.8$ kV-μs. We further choose its width as $T_1 = 0.25$ μs so that $V = 3.2$ kV, and the barrier is positioned between $6.75T_b$ and $7.0T_b$. The stationary barrier is represented by a red-filled box while the moving barrier is represented by an unfilled box with an arrow inside pointing to the direction of its motion. After one booster cylce, we see in bottom plot of Fig. 6 that all the particles of the first batch go past the left edge of the moving barrier and some are reflected by the stationary barrier. At this moment, a second batch is injected in the region between $5.0T_b$ and $6.0T_b$. We alternate the color of successive batches so that their trajectories can be followed easily. The six vertical dashes lines divide the circumference of the Main Injector into 7 regions each of which is of length T_b or one booster-batch long. Two thousand macroparticles are used to simulate each booster batch.

Successive batch injection continues. The situation of one booster cycle after the injection of the 12th batch between $0.0T_b$ and $1.0T_b$, or 12 booster cycles after the injection of the first batch, is shown in the top plot of Fig. 7. We need to wait until another booster cycle later, the bottom plot, to allow all the particles to drift inside the designated momentum spread. This is now the time to perform adiabatic capturing and acceleration. Thus an injection time of 13 booster cycles or 0.87 s will be required. We see empty spaces between successive batches in both plots of Fig. 7, indicating an increase in longitudinal emittance. The ratio of final emittance to initial emittance will be slightly larger than $r_e = 1.21$ given by Eq. (5.4) because of the finite number of injections here. For the same reason, the ratio of

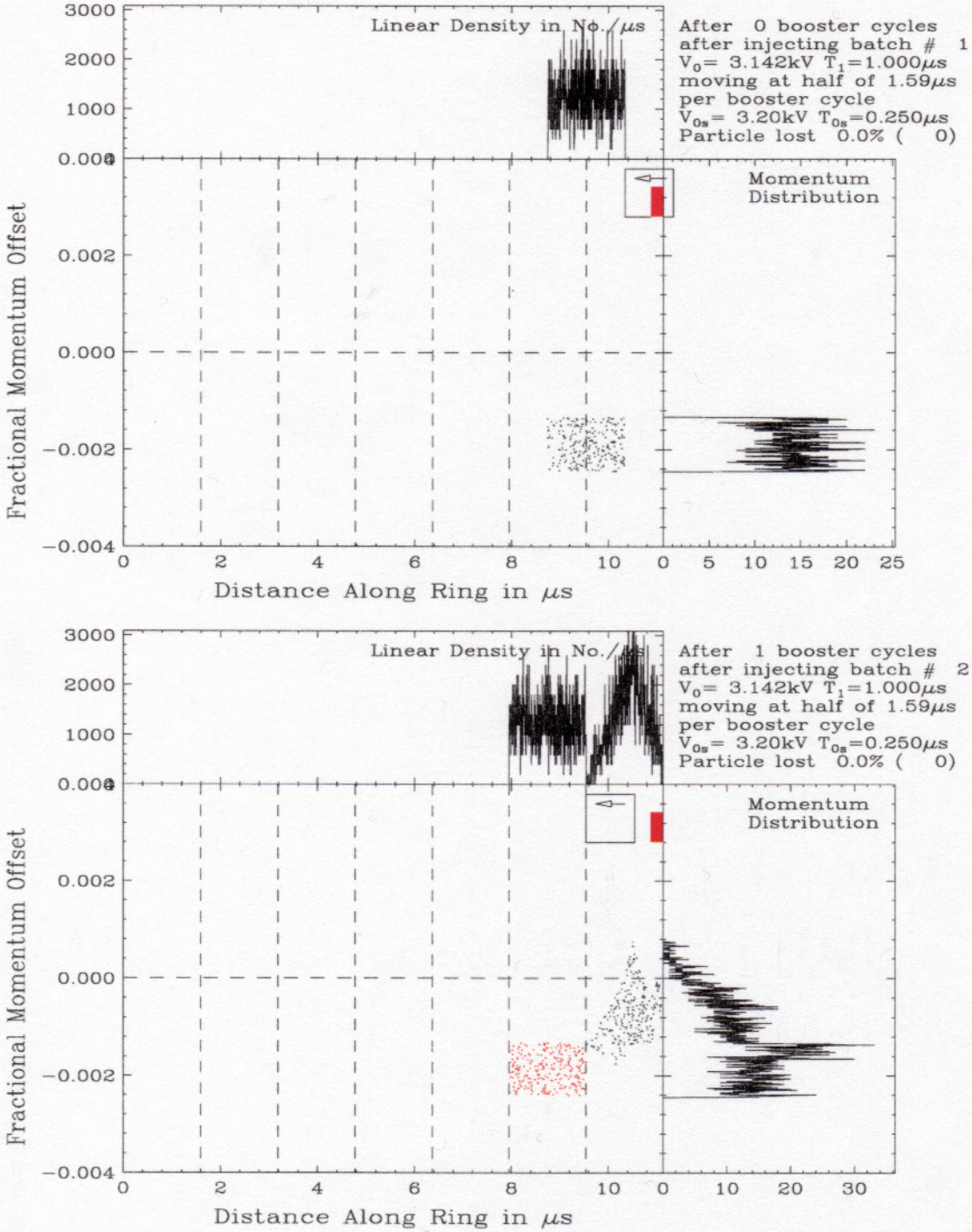

Figure 6: (color) Top: First batch (black) is injected between $5.5T_b$ and $6.5T_b$ with the right side touching the left side of the moving barrier, illustrated as a unfilled box with an arrow. Bottom: After one booster cycle, all particles in the first batch have just cleared the left side of the moving barrier, which is at $6.0T_b$. The second batch (red) is now injected between $5.0T_b$ and $6.0T_b$. Moving barrier has width $T_1 = 1.0\,\mu$s and strength $V = 3.1421\,$kV. Vertical dashes lines are spaced at T_b.

final linear density to initial linear density will be slight less than $r_d = 2.0$ given by Eq. (5.5).

The simulation is repeated with the width of the moving barrier reduced to $T_1 = 0.5$ μs; the strength is therefore increased to $V = 6.2842$ kV. Because of the narrower width of the barrier, at the injection of the first batch, the left side of the barrier can be placed at $6.7T_b$, correspondingly the first batch between $5.7T_b$ and $6.7T_b$, without particle loss. Successive batch injections are carried on in the same way. The top plot of Fig. 8 shows the situation of one booster cycle after the injection of the 12th batch at position between $0.2T_b$ and $1.2T_b$, or 12 booster cycles after the injection of the first batch. Compared with the top plot of Fig. 7, all particles are now inside the designated momentum spread. Adiabatic capture can begin immediately. Thus, one booster cycle can be saved. However, the longitudinal spread is contained within $6.2T_b$, which is not much less than the $\sim 6.5T_b$ in the bottom plot of Fig. 7. Thus the emittance ratio and linear-density ratio should be roughly the same as in the case of the 1 μs moving barrier.

6.2 DISCUSSIONS

(1) It is nontrivial to compute the initial positioning of the moving barrier relative to the position of the stationary barrier. A sufficient condition is that a particle will not be seeing the two barriers in the same revolution turn. This implies that a particle should emerge from the moving barrier before entering into the stationary barrier. Particle 2 at the lower right corner of the batch will emerge first from the moving barrier. At the critical condition, it is easy to compute using Eq. (2.3) that it takes the particle $N_2 = 3119$ turns to pass through the moving barrier of width 1.0 μs. At this moment, the barrier moves the the left a distance $N_2\dot{T}_2T_0 = 0.26T_b$. Thus at the injection of the first batch, the right side of the moving barrier should be $0.26T_b$ to the left side of the left edge of the stationary barrier. Or, the left side of the moving barrier should be at location $[7 - 0.26 - (0.25 + 1.0)/T_b]T_b = 5.95T_b$ along the ring. But actually we can place it at $6.5T_b$ without any particle loss. This is because we can allow the particle to interact with both barriers in the same revolution turn, provided that no particle will be energetic enough to penetrate the stationary barrier or to go outside the designated final energy spread of the beam.

(2) Barrier waves are usually used to to confine a beam so that it will stay within a designated region along the accelerator ring. The integrated sizes of the barriers need not be

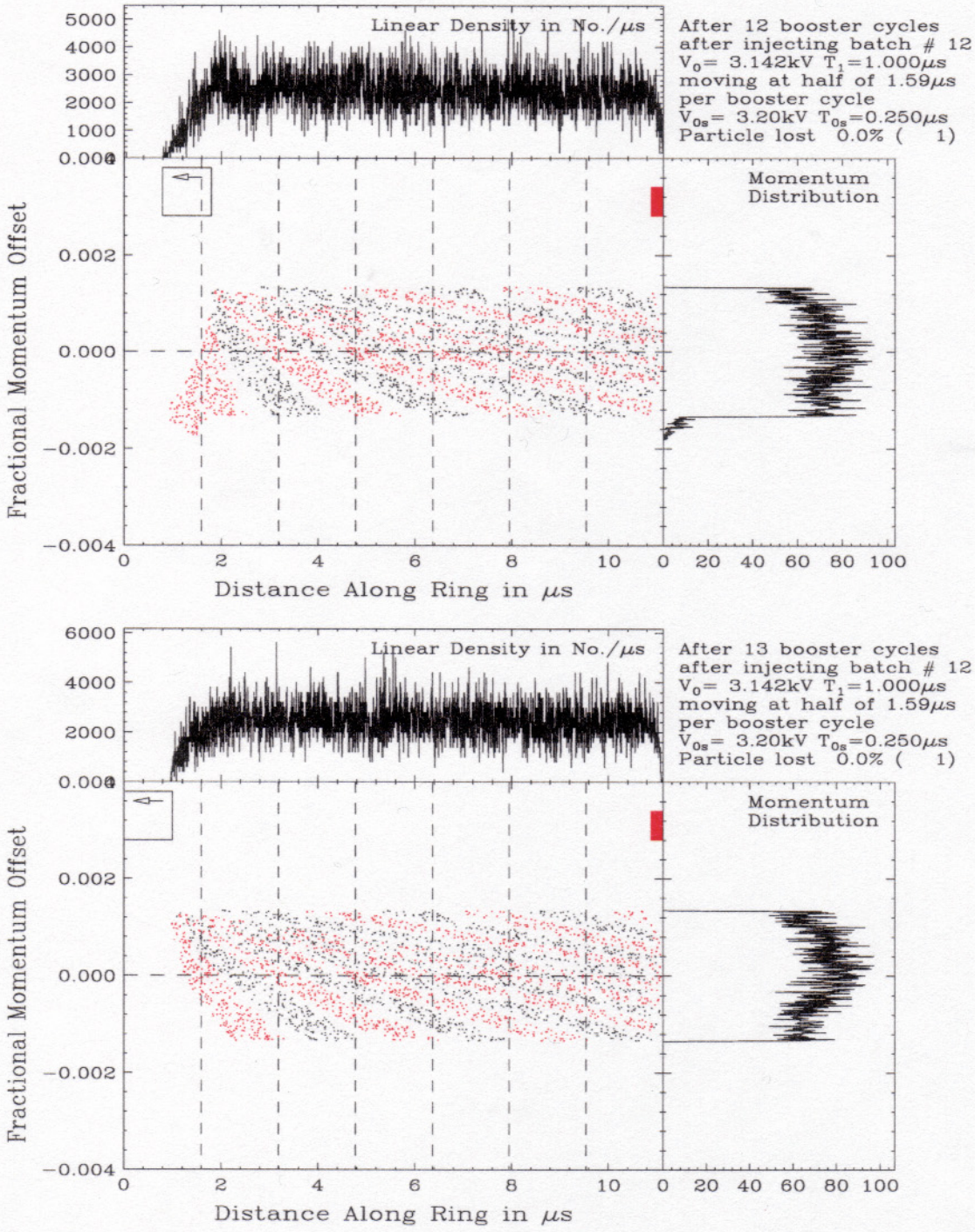

Figure 7: (color) Continuing the injection from Fig. 7. Top: One booster cycle after the injection of the 12th batch between $0.0T_b$ and $1.0T_b$, or 12 booster cycles after the injection of the first batch. Bottom: Another booster cycle later or 13 booster cycles after the injection of the first batch. All particles are within the designated final momentum spread and adiabatic capture can begin.

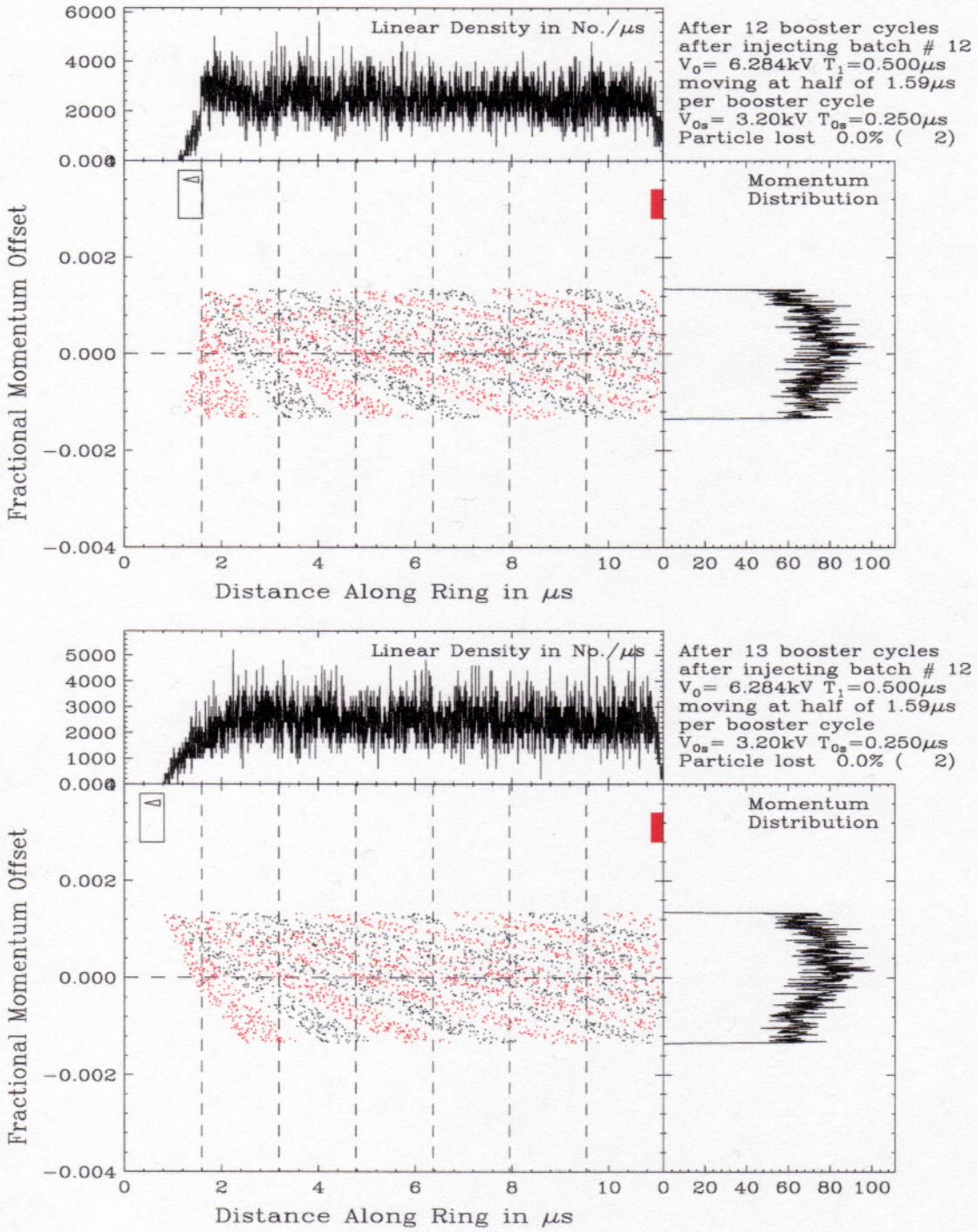

Figure 8: (color) Same as Fig. 7, but with the width of the moving barrier reduced to 0.5 μs and strength increased to 6.2842 kV. At injection of first batch, left side of barrier was placed at $6.7T_b$. Top: One booster cycle after the injection of the 12th batch between $0.2T_b$ and $1.2T_b$, or 12 booster cycles after the injection of the first batch. Bottom: Another booster cycle later.

accurate as long as they are large enough to confine the particles of the highest and lowest energies. However, this is not true here. Although the injection process does not depend on the shape of the moving barrier, its integrated size has to be accurate in order to have the final positive and negative energy spreads be equal and opposite. Otherwise, after reflection by the stationary barrier, the positive energy spread will be modified, resulting possibly in an increase in the longitudinal emittance. Here, we would like to study the effect of such an error. The top plot of Fig. 9 shows the situation when VT_1 is 10% larger than its critical value, while the width of the barrier is kept at $T_1 = 0.5$ μs. The plot shows the moment one booster cycle after the injection of the 12th batch, and should be compared with the top plot of Fig. 8. For a stronger moving barrier, most particles will emerge the barrier at higher energies. This is evident for the particles with the least energy in the batch. We see a final negative momentum spread of $\delta_{f2} = -1.206 \times 10^{-3}$, which is about 10% less negative than the -1.344×10^{-3} in the top plot of Fig. 8. Actually, the negative normalized final momentum spread is given by

$$\bar{\delta}_{f2} = \frac{1}{2} - \sqrt{\left(\frac{1}{2x} + \bar{\Delta}\right)^2 - A}\ , \tag{6.6}$$

where the normalized initial full momentum spread is $\bar{\Delta} = \sqrt{2} - 1$. Here, A is proportional to VT_1 and its critical value is $1/(4x^2)$. Putting in $x = \frac{1}{2}$ and $A = 1.1$, we arrive at the 10% reduction as given by the simulation. For particles of the highest energies, many of them will not be able to make their way out of the enhanced moving barrier, resulting in beam loss. Some of the loss is evident in the plot at the location of the moving barrier. The total loss recorded is 2555. There are 2000 macroparticles in each batch, giving a loss of 10.6%.

The situation of a reduction of VT_1 by 10% from its critical value is shown in the bottom plot of Fig. 9. Now all particles will emerge from the moving barrier earlier and their energies are therefore reduced. According to Eq. (6.6), $\bar{\delta}_{f2}$ will be 9.8% more negative. The simulation gives 9.2%. We see that final momentum offset of particles with the highest energy are affected most. According to Eq. (5.2), $\bar{\delta}_{f1}$ will be reduced by 63%, which agrees with the result of the simulation. However, the final positive momentum spread is determined by the negative final momentum spread after the reflection by the stationary barrier. Thus, the final momentum spread actually increases by 9.8%, about the amount of the error in VT_1. The loss recorded is 11, or 0.045%. This loss comes from the reflection by the stationary barrier. Some of these particles have energies high enough that their left-drift velocities are higher than that of the moving barrier. Eventually, some particles catch up with the moving barrier and get lost.

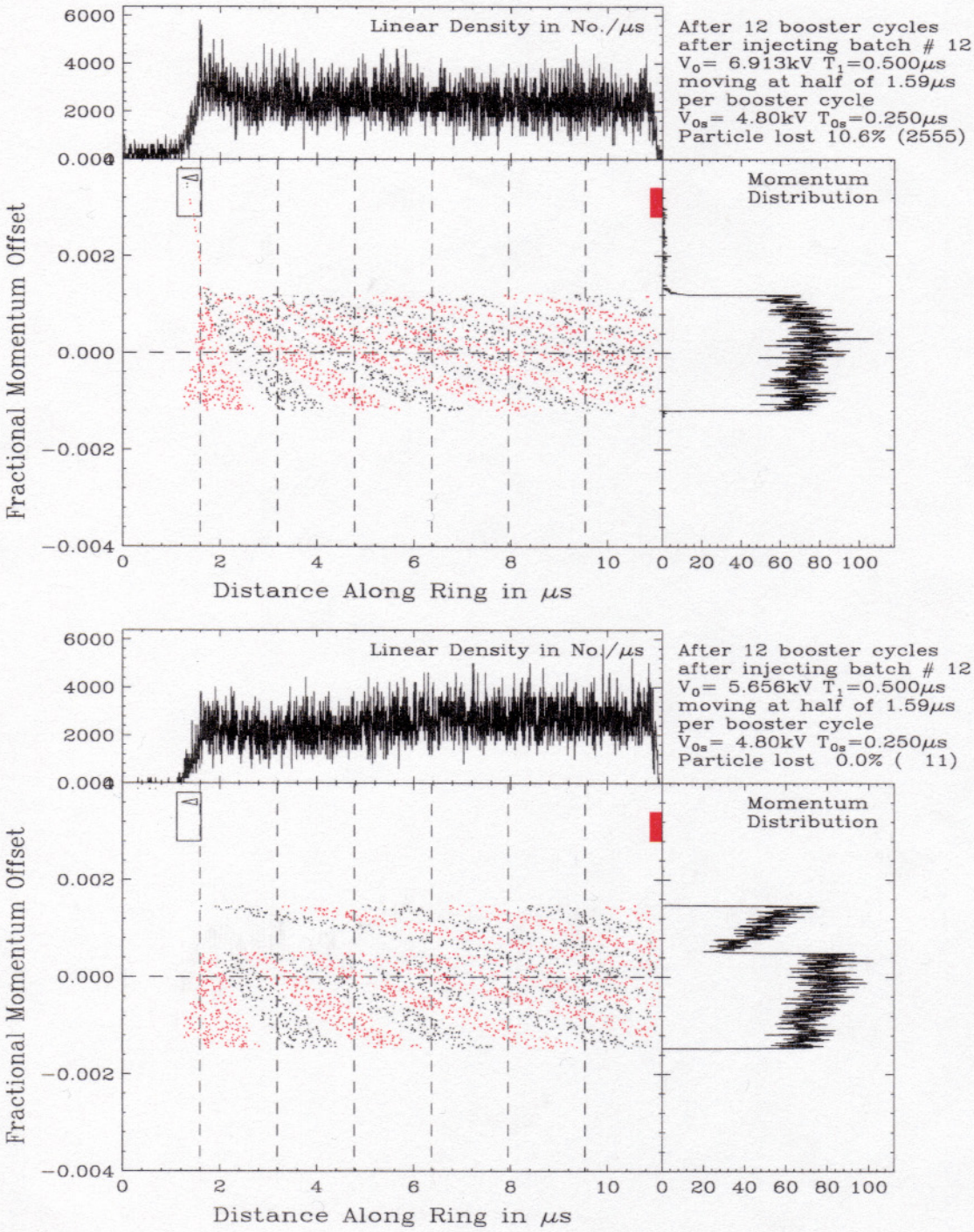

Figure 9: (color) Plots showing the moment one booster cycle after the injection of the 12th batch. Everything is the same as in the top plot of Fig. 8, except VT_1 of the moving barrier is increased by 10% in the top plot and decreased by 10% in the bottom plot. The width of the moving barrier is kept fixed at $T_1 = 0.5\,\mu$s.

(3) This injection method requires only two barriers, one moving and one stationary. Unfortunately, they are of the same sign. In practice, one must also introduce barriers of the opposite sign to cancel the charge accumulation. Therefore, space along the ring must be available for their introduction. This may shorten the space available for successive batch injections. Therefore, we may require narrow barriers (less than 0.5 μs) with high voltages ($\gtrsim$ 6 kV) to ensure the injection of 12 booster batches.

6.3 ADIABATIC CAPTURE

We want to examine the adiabatic capture of a coasting beam in the Main Injector at injection. Here, we set the criterion that the relative change in bucket height or bucket area A_b should be much slower than the synchrotron angular frequency ω_s, or

$$\omega_s \gg \frac{1}{A_b}\frac{dA_b}{dt} \ . \tag{6.7}$$

Bunch area is proportional to $\sqrt{V_{\rm rf}}$ and ω_s is also proportional to $\sqrt{V_{\rm rf}}$, where $V_{\rm rf}$ is the rf voltage. Let $a = \omega_s/\sqrt{V_{\rm rf}}$. Then

$$a \gg \frac{1}{2V_{\rm rf}^{3/2}}\frac{dV}{dt} \ , \tag{6.8}$$

or

$$at \gg \frac{1}{\sqrt{V_{\rm rf}(t)}} + C \ , \tag{6.9}$$

where C is a constant. We cannot start from $V_{\rm rf} = 0$, because the constant C will become infinite. So we start from $V_{\rm rf} = V_1$ at $t = 0$ and end at $V_{\rm rf} = V_2$ at $t = t_2$, giving $C = 1/\sqrt{V_1}$. Define ω_{s1} as the initial angular synchrotron frequency (at $V_{\rm rf} = V_1$). Then

$$\omega_{s1}t \gg \sqrt{\frac{V_1}{V(t)}} + 1 \tag{6.10}$$

If good adiabaticity requires the relative rate of change of bucket area to be $1/n$ of the synchrotron angular frequency, we obtain the rf voltage curve

$$\sqrt{\frac{V_{\rm rf}(t)}{V_1}} = \frac{1}{1 - \omega_{s1}t/n} \ . \tag{6.11}$$

For example, if we start from $V_1 = 5$ kV and end at $V_2 = 500$ kV, the capture time will be $t_2 = 23.28$ ms when $n = 10$.

In the injection scheme discussed here, if the injected booster batch has a half energy spread of 5 MeV, after exiting the moving barrier, the half spread becomes 12 MeV. We want to capture the beam into buckets with rf harmonic $h = 588$. There are 3 variables: V_1, V_2, and n. It appears that n has to be larger than 10. In fact $n = 15$ is a more appropriate number. The final rf voltage cannot be too small because the initial half energy spread is 12 MeV already. The initial bunch area is $2\Delta E_{f1} T_0/h = 0.4544$ eV-s. For such a bucket area, a rf voltage of $V_{\rm rf} = 268.3$ kV is required. For this reason, we set $V_2 = 500$ kV. This rf voltage will establish a bucket with area 0.620 eV-s and half height 23.16 MeV. On the other hand, a bunch of area 0.4544 eV-s will have half length 7.28 ns and half height 21.65 MeV. Thus, V_2 cannot be much less than 500 kV. Then, V_1 becomes the only variable. The capture time for a given V_1 and V_2 can be read off easily from Fig. 10. As an example, $V_1 = 20$ kV,

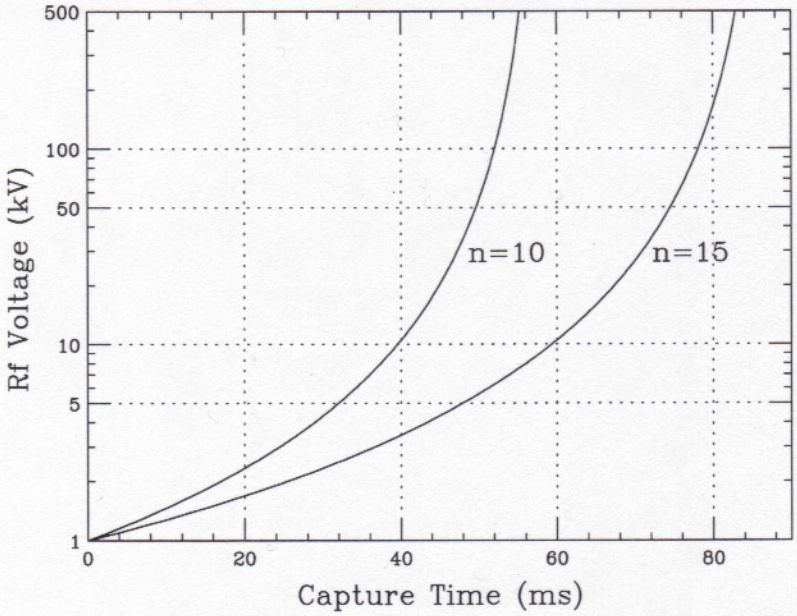

Figure 10: Plot of capture time in ms for various initial and final rf voltages V_1 and $V_2 = 500$ kV. The relative rate of change of bucket area is taken as 1/n of the angular synchrotron frequency, where $n = 10$ or 15.

$V_2 = 500$ kV, and $n = 15$ lead to a capture time of 15.52 ms or 1393 turns. Changing n to 10 will reduce the capture time to 10.35 ms or 929 turns.

Simulations of adiabatic capture are performed from various initial rf voltage V_1 to the final $V_2 = 500$ kV. The results are shown in Fig. 11 for the adiabaticity $n = 10$ and in Fig. 12 for the adiabaticity $n = 15$. It appears that the capture is acceptable even if we start with rf voltage $V_1 = 50$ kV. The capture time will be 5.6 ms at $n = 10$ and 8.4 ms

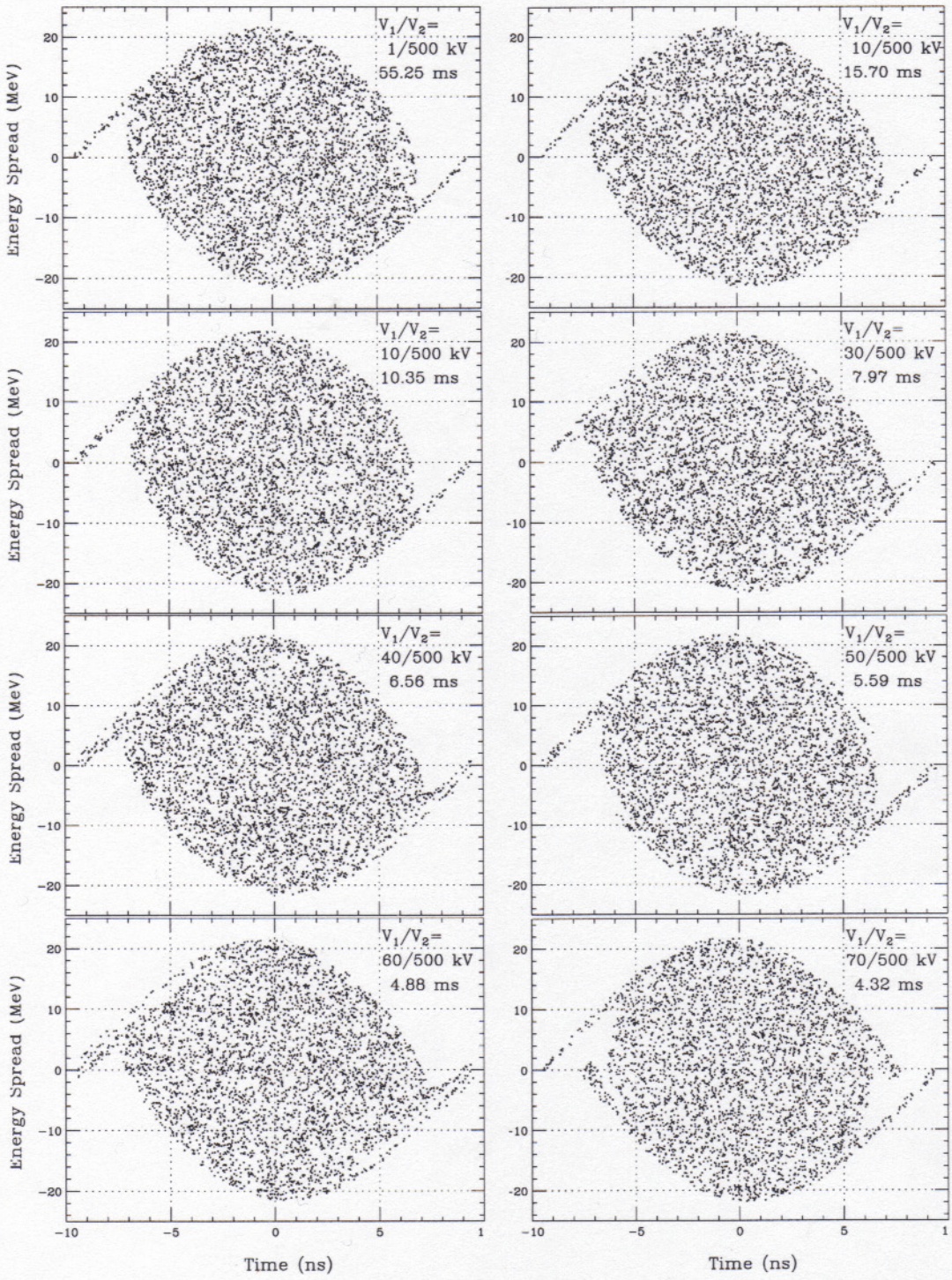

Figure 11: Plot of a 53 MHz bunch in the longitudinal phase space after adiabatic capture starting from various initial rf voltage V_1 to the final $V_2 = 500$ kV. Adiabaticity is fixed at $n = 10$ and the initial bunch area is $2\times12\times11.134/588 = 0.4544$ eV-s. At $V_2 = 500$ kV, final half bunch height is 21.65 MeV and half width 7.28 ns.

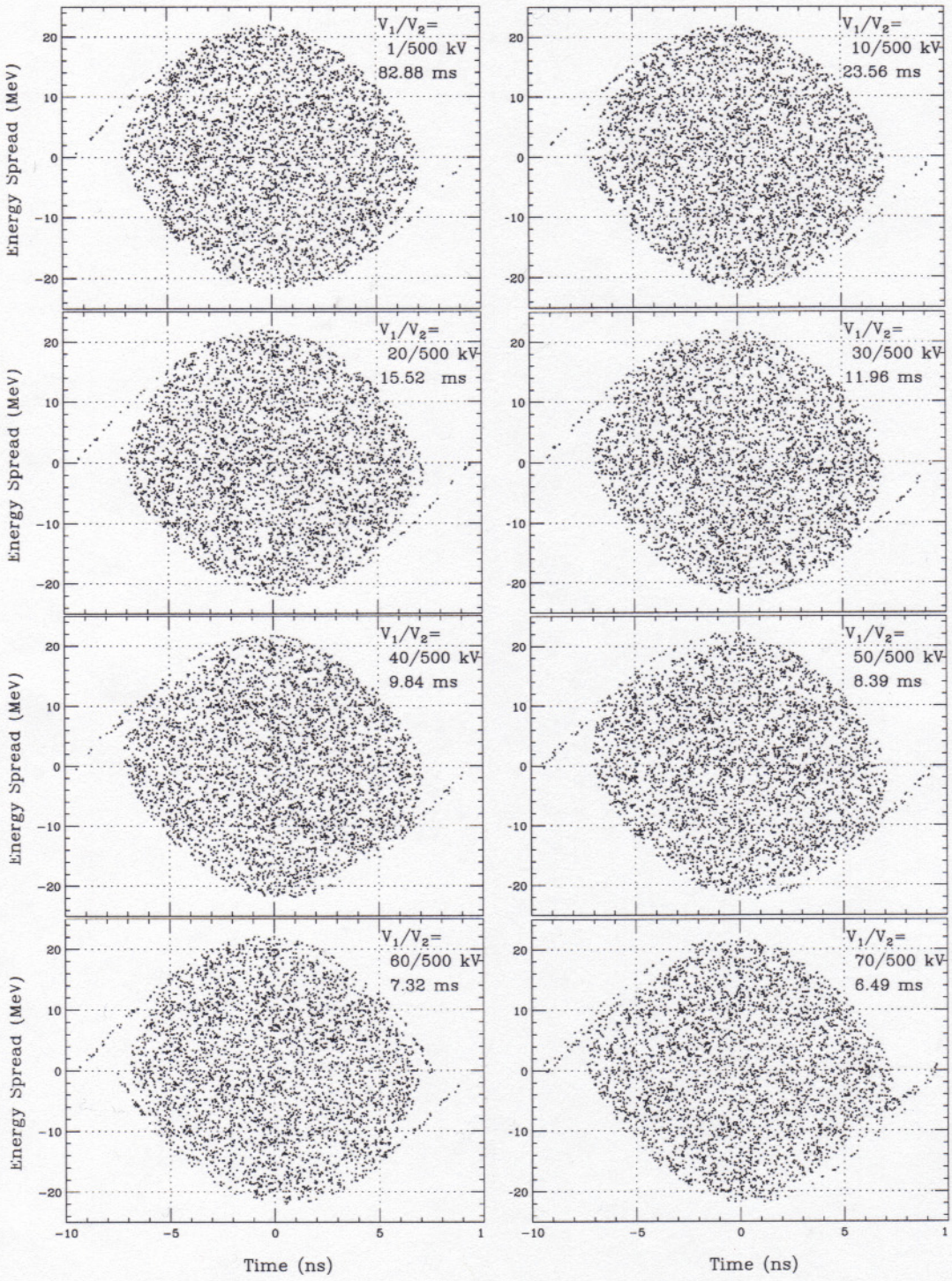

Figure 12: Plot of a 53 MHz bunch in the longitudinal phase space after adiabatic capture starting from various initial rf voltage V_1 to the final $V_2 = 500$ kV. Adiabaticity is fixed at $n = 15$ and the initial bunch area is $2\times12\times11.134/588 = 0.4544$ eV-s. At $V_2 = 500$ kV, final half bunch height is 21.65 MeV and half width 7.28 ns.

at $n = 15$. In Fig. 13, we give a closer look at the captures again from $V_1 = 50$ kV to $V_2 = 500$ kV at adiabaticity $n = 10$ in the top plot and $n = 15$ in the bottom plot. We also superimpose as solid green curves the boundaries of the bunches with area 0.4544 eV-s that are matched to the rf voltage of $V_2 = 500$ kV. Particles outside the green curves are considered lost eventually. Here, we see a 6.0% loss for $n = 10$ and only 3.0% loss for $n = 15$. We can conclude that an adiabatic capture time of ~ 10 ms will be quite adequate using $n = 15$.

7 BEAM LOADING

Because of the high beam current, beam loading voltage induced in the Main Injector rf cavities can become a serious problem. In fact, beam loading represents the most series problem in slip-stacking. A bunch at the 53 MHz rf voltage (harmonic $h = 588$) containing 6.0×10^{10} protons carries a charge of $q = 9.61$ nC. If the bunch is short, it can be approximated by a macroparticle, which will induce an instantaneous beam loading voltage

$$V_{b0}(t) = \frac{q\omega_r R_L}{Q_L} e^{-i\bar{\omega}_r t - \omega_r t/(2Q_L)} \tag{7.1}$$

across the cavity gap, where R_L, Q_L, and $\omega_r/(2\pi)$ are, respectively, the loaded shunt impedance, loaded quality factor, and resonant frequency of the cavity. The quality-factor shifted resonant angular frequency is $\bar{\omega}_r = \omega_r\sqrt{1 - 1/(4Q_L^2)}$. For a typical Main Injector rf cavity, $R_L/Q_L = 100\ \Omega$. The *unloaded* quality factor is $Q = 5000$. For the rf system of a proton ring, the generator coupling coefficient is close to $\beta = 1$. Thus, $Q_L \approx 2500$. Bunch spacing is $\tau = T_0/h$. The loaded decay decrement between successive bunches is therefore $\delta_L = \omega_r\tau/(2Q_L) = \pi/Q_L$. If we neglect detuning and assume the ring completely full, the total beam loading voltages left by the preceding bunches add up as a geometric series to give

$$V_b = \frac{q\omega_r R_L}{Q_L}\frac{1}{1 - e^{-\pi/Q_L}}\ . \tag{7.2}$$

For bunches containing 6.0×10^{10} protons each, this beam loading voltage becomes 0.254 MV. When the bunch intensity is doubled, this becomes[¶] 0.508 MV, which is larger than the nominal desired gap voltage of 100 kV per cavity. Note that the actual beam loading voltage

[¶]This value differs from the ~ 3 MV predicted in Ref. [10]. The difference may come from the use of (1) an incorrect decay decrement of $\pi/(2Q)$ and (2) the unloaded quality factor instead of the loaded.

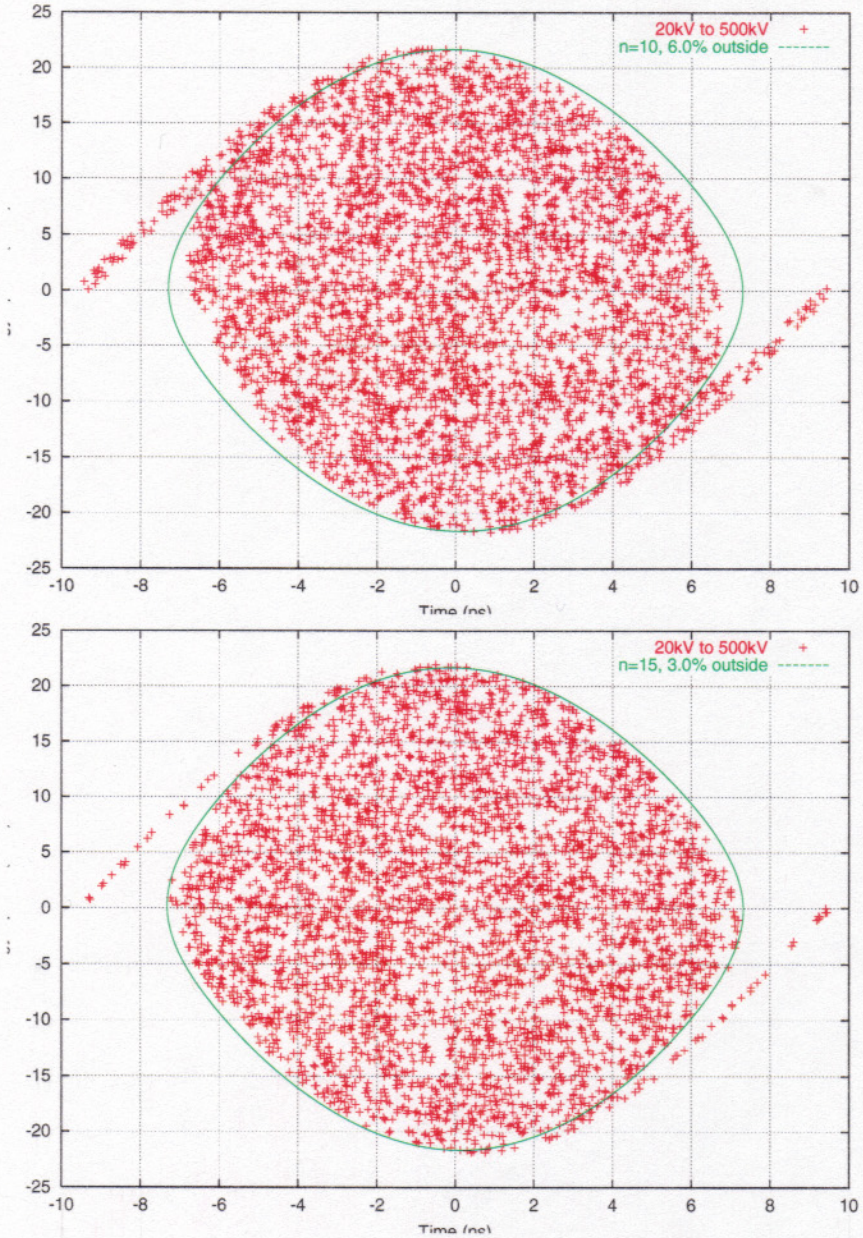

Figure 13: (color) Adiabatic capture starting from $V_1 = 50$ kV to $V_2 = 500$ kV with adiabaticity $n = 10$ in the top plot and $n = 15$ in the bottom plot. The solid green curve in each plot represents the boundary of the bunch of 0.4544 eV-s (initial area) matched to the rf voltage of V_2. Particles outside the curve may be lost eventually. The loss is 6.0% for $n = 10$ and reduces to 3.0% at $n = 15$.

seen by the beam particle should be less because (1) the bunch has a longitudinal spread and is not a macroparticle, (2) there are unfilled buckets, and (3) there is a detuning.

The following methods were proposed in Ref. [10] to control the beam loading voltage in slip-stacking:

1. Tuning all cavities to the nominal 8 GeV frequency.
2. Using only 2 or 4 of the cavities to produce the required rf voltage and de-Qing the remaining cavities. One simple technique that may de-Q the cavities by a factor of 3 is to turn off the screen voltage to reduce the tube plate resistance.
3. Feed-forward the signal of the wall current monitored at a resistive-wall gap to the cavity drivers. Experience at the Main Ring expects to achieve a 10-fold reduction in the effective wall current flowing into the cavities.
4. Feedback on all the cavities. A signal proportional to the gap voltage is amplified, inverted, and applied to the driver amplifier. Based on experience in the Main Ring and results achieved elsewhere, a 100-fold reduction can be achieved.

In our continuous multiple injection scheme using barriers, the booster bunches contained in the batch at injection will be made very long so that the momentum spread can be reduced. These bunches start debunching almost immediately. For a completely uniformly distributed beam, there is no 53 MHz rf component and therefore no beam loading at all. Here, although the distribution is not uniform (see, for example, Fig. 8), we expect the 53 MHz rf component of the beam will be very much less if the bunches are concentrated as macroparticles. Thus, the beam loading voltage should be very much less than what will be experienced during slip-stacking. In addition, for the second control effect stated above, all cavities can be de-Qed, since no 53 MHz rf will be necessary during successive injections. If all the above control efforts are successful, beam loading should not pose a problem any more.

APPENDIX

In this appendix, we are going to show that the injection process discussed in this paper depends only on the integrated barrier voltage and does not depend on the shape of the barrier. Thus, whenever VT_1 appears, we can make the substitution

$$VT_1 = \int V(\tau)d\tau \ , \tag{A.1}$$

where $V(\tau)$ is a general barrier wave.

The Hamiltonian describing the longitudinal motion of a particle of charge e interacting with a *stationary* barrier wave can be written as

$$H = -\frac{1}{2}|\eta|\delta^2 - \frac{e}{\beta^2 E T_0}\int_0^\tau V(\tau')d\tau' \ , \tag{A.2}$$

so that the equations of motion are

$$\frac{d\tau}{dt} = -|\eta|\delta \ , \tag{A.3}$$

$$\frac{d\delta}{dt} = \frac{eV(\tau)}{\beta^2 E T_0} \ . \tag{A.4}$$

Here, δ and τ are, respectively, the fractional momentum offset and arrival time advance of the particle. For simplicity, we have also restricted ourselves to operation below transition.

The particle has initial fractional momentum offset δ_{i1} at time $t = 0$ when it starts entering the barrier. Then from the Hamiltonian

$$\frac{1}{2}|\eta|\delta_{i1}^2 = \frac{1}{2}|\eta|\delta^2(\tau) - \frac{e}{\beta^2 E T_0}\int_0^\tau V(\tau')d\tau' \ . \tag{A.5}$$

We can also starts from the equations of motion,

$$\frac{d}{dt}\frac{d\tau}{dt} = -\frac{|\eta|eV(\tau)}{\beta^2 E T_0} \ . \tag{A.6}$$

Multiplying by $2d\tau/dt$,

$$\frac{d}{dt}\left(\frac{d\tau}{dt}\right)^2 = -\frac{2|\eta|eV(\tau)}{\beta^2 E T_0}\frac{d\tau}{dt} \ , \tag{A.7}$$

$$\left(\frac{d\tau}{dt}\right)^2 = \left(\frac{d\tau}{dt}\right)_{i1}^2 - \int_0^\tau \frac{2|\eta|eV(\tau')}{\beta^2 E T_0}d\tau' \ . \tag{A.8}$$

Substituting the phase equation, we obtain again

$$\delta^2(\tau) = \delta_{i1}^2 - \int_0^\tau \frac{2eV(\tau')}{|\eta|\beta^2 ET_0} d\tau' \ . \tag{A.9}$$

Now the barrier is moving at the rate $\dot{T}_2$ to the left. When the particle is at time advance τ, it is seeing the barrier wave at time advance $\tilde{\tau} = \tau + \dot{T}_2 t$. The Hamiltonian changes to

$$H = -\frac{1}{2}|\eta|\delta^2 - \frac{e}{\beta^2 ET_0}\int_0^{\tau+\dot{T}_2 t} V(\tau')d\tau' \ , \tag{A.10}$$

and the energy equation becomes

$$\frac{d\delta}{dt} = \frac{eV\left(\tau + \dot{T}_2 t\right)}{\beta^2 ET_0} \ . \tag{A.11}$$

Let us go to the rest frame of the barrier. The phase advance for the particle becomes $\tilde{\tau}$ and the phase equation is

$$\frac{d\tilde{\tau}}{dt} = \frac{d\tau}{dt} + \dot{T}_2 = -|\eta|\left(\delta - \frac{\dot{T}_2}{|\eta|}\right) \ . \tag{A.12}$$

We can write the energy equation as

$$\frac{d}{dt}\left(\delta - \frac{\dot{T}_2}{|\eta|}\right) = \frac{eV(\tilde{\tau})}{\beta^2 ET_0} \ . \tag{A.13}$$

In other words, in the rest frame of the moving barrier, the Hamiltonian becomes

$$H = -\frac{1}{2}|\eta|\tilde{\delta}^2 - \frac{e}{\beta^2 ET_0}\int_0^{\tilde{\tau}} V(\tau')d\tau' \ , \tag{A.14}$$

where

$$\begin{aligned} \tilde{\tau} &= \tau + \dot{T}_2 t \ , \\ \tilde{\delta} &= \delta - \frac{\dot{T}_2}{|\eta|} \end{aligned} \tag{A.15}$$

are the new canonical variables. We therefore have the solution

$$\delta_{f1} - \frac{\dot{T}_2}{|\eta|} = -\sqrt{\left(\delta_{i1} - \frac{\dot{T}_2}{|\eta|}\right)^2 - \frac{2}{|\eta| T_0 \beta^2 E}\int_0^{\tau_f} V(\tau')d\tau'} \ , \tag{A.16}$$

where τ_f is the total width of the barrier and δ_{f1} is the fractional momentum offset of the particle on exiting the barrier. Here, the negative sign in front of the square root sign has been chosen, because as $\tau_f \rightarrow 0$, on must have $\delta_{f1} \rightarrow \delta_{i1}$, noting that $\delta_{i1} < 0$. Equation (2.7) is just a special case of Eq. (A.16) when the barrier is of square shape. Starting from Eq. (2.7), we see that VT_1 comes about as one variable. Thus, the replacement in Eq. (A.1) can be made in all the equations that follow.

References

[1] *Run II Handbook*, Fermilab Report, http://www-bd.fnal.gov/runII/index.html

[2] *Plan for Tevatron Run IIb*, Fermilab Report, http://cosmo.fnal.gov/run2b/Documents/TDR/tdr.pdf

[3] C. Ankenbrandt, *"SLIP-STACKING": A New Method of Momentum-Stacking*, Fermilab Report FN-352, 1981; F.E. Mills, *Stability of Phase Oscillations under two Applied Frequencies*, BNL Internal Report AADD 176, 1971.

[4] D. Boussard and Y. Miszumachi, IEEE Trans. Nucl. Sc. **NS-26**, 3623 (1979); J.P. Delahaye, P. Lefevre, and J.P. Riunaud, IEEE Trans. Nucl. Sc. **NS-26**, 3565 (1979).

[5] S. Machida, private communication.

[6] K.Y. Ng, *Multiple Injection with Barrier Buckets*, Proceedings of 1997 Particle Accelerator Conference, Vancouver, B.C., Canada, 12-16 May 1997, p.1003; K.Y. Ng, *Injection of JHP Main Ring Using Barrier Buckets*, Fermilab Report FN-654, 1997.

[7] M. Blaskiewicz, J.M. Brennan, T. Roser, K. Smith, R. Spitz, A. Zaltsmann, M. Fujieda, Y. Iwashita, A. Noda, M. Yoshii, Y. Mori, C. Ohmori, Y. Sato, *Barrier Cavities in the Brookhaven AGS*, Proceedings of the 1999 Particle Accelerator Conference, New York, 1999, p.2280; M. Fujieda, Y. Iwashita, A. Noda, Y. Mori, C. Ohmori, Y. Sato, M. Yoshii,, M. Blaskiewicz, J.M. Brennan, T. Roser, K. Smith, R. Spitz, A. Zaltsmann, *Magnetic Alloy Loaded Rf Cavity for Barrier Bucket Experiment at the AGS*, Proceedings of the 1999 Particle Accelerator Conference, New York, 1999, p.857;

[8] J. Griffin, *Momentum Stacking in the Main Injector using Longitudinal Barriers*, Fermilab Internal Report, 1996.

[9] J. Griffin, private communication.

[10] Shekhar Shukla, John Marriner, and James Griffin, *Slip Stacking in the Fermilab Main Injector*, Proceedings of Summer Study on the Fututre of Particle Physics, Snowmass, CO, July 1-20, 2001.